Science in China Series E: Technological Sciences

Springer

www.scichina.com
tech.scichina.com
www.springerlink.com

Deposition of aerosol in a laminar pipe flow

LUO XiaoWei† & YU SuYuan

Institute of Nuclear Energy and New Energy Technology, Tsinghua University, Beijing 100084, China

In a laminar pipe flow, thermophoretic deposition occurs when the temperature of the pipe wall is less than the temperature of the fluid. For a horizontal pipe, gravity has a significant effect on the deposition of aerosol. Due to the laminar flow of gas fluid, a lift force is imposed on the particle and could affect the deposition of aerosol. In the present work, we considered the influences of various factors on the deposition of aerosol, including diffusion and convection, thermophoresis, gravitational settling and the lift force effect. The revised semi-implicit method for pressure-linked (SIMPLER) was employed to solve the aerosol transport equation. The deposition efficiency of aerosol in a pipe was obtained and the concentration distribution of aerosol at an arbitrary cross-section of pipe was given. The results reveal that when gravitational settling was considered the deposition efficiency had a minimum, corresponding to the penetration efficiency having a maximum. For large particles, the deposition of aerosol was dominated by external forces, and the critical particle trajectory method (CPTM) was used to analyze the deposition of aerosol with the action of thermophoretic force and gravity. The result from CPTM coincided very well with the result from SIMPLER.

aerosol, thermophoresis, gravitational settling, deposition

1 Introduction

When the particles flow in a pipe are carried by gas fluid, the particles are deposited on the pipe wall due to various factors. This phenomenon occurs in many industrial processes, such as air cleaning, aerosol sampling, hot-gas filtration, coal combustion and microcontamination. For the deposition of aerosol in a pipe flow, based on the flow state of the fluid, the deposition can be classified as either deposition in a laminar flow or deposition in a turbulent flow. For fluid in a laminar flow, the main factors that influence the deposition of particles include Brownian force, gravity, thermophoretic force and lift force. For fluid in a turbulent flow, the main influencing factors include Brownian force, gravity, thermophoretic force, turbulent diffusion, turbulent colli-

Received August 20, 2007; accepted January 25, 2008
doi: 10.1007/s11431-008-0140-7
†Corresponding author (email: xwluo@tsinghua.edu.cn)
Supported by the National Natural Science Fundation of China (Grant No. 50476010) and the Tsinghua University Key Personnel Support Plan (Grant No. 05321400)

sion and lift force. For each deposition mechanism, many researchers have carried out much theoretical and experimental investigation. Ounis et al.[1−3] compared the effects of Brownian and turbulent diffusion, and computed the diffusion of submicron particles in a simulated turbulent channel flow. Li and Ahmadi[4,5] performed a series of simulations on transport and deposition of Brownian and inertial particles in a duct flow. Hinds[6] gave a deposition efficiency formula for laminar pipe flow.

When there is a temperature gradient, the aerosol particles migrate from high temperature to low temperature zones. This phenomenon is called thermophoresis. In 1962, based on Navier-Stokes-Fourier theory Brock[7] gave the thermophoretic force by hydrodynamic analysis. Talbot et al.[8] used the experimental datum to correct Brock's equation. Brock and Talbot's equations are only applicable for $K_n < 2$ ($K_n = \lambda/R_p$). In 1995, Tasi and Lu[9] designed a plate-to-plate thermophoretic precipitator to test the collection efficiency, and found that the thermophoretic force proposed by Talbot et al. was accurate. For $K_n > 2$, their experimental data for sodium fluorescein particles, however, showed that collection efficiency decreases as particle diameter decreases. This trend could not be predicted by the thermophoretic model of Talbot et al. Li and Davis[10,11] reviewed different theoretical formulations of thermophoresis and reported their experimental results. The results indicated that the normalized thermophoretic force has a peak in the region of $K_n > 2$, and decreases beyond this point as K_n increases. Earlier, Wood[12] and Cha and McCoy[13] pointed out that a peak thermophoretic force occurred for certain particle diameters, and gave the Cha-McCoy-Wood formula to calculate the thermophoretic force. He and Ahmadi[14] adopted the experimental results of Li and Davis to test the Cha-McCoy-Wood equation, and found that it underestimated the thermophoretic force magnitude. Based on experimental results, He and Ahmadi corrected the Cha-McCoy-Wood equation. Lin and Tsai[15] provided a detailed discussion of the effect of the entrance of a pipe on the thermophoretic deposition, and gave a formula for a fully developed flow and a developing flow. In 2004, Tsai et al.[16] validated various thermophoretic deposition formulas by experimental data, and found that the Talbot equation had the best fit with the experiments.

Yiantsios and Karabelas[17] analyzed the influence of gravity on the deposition of particles, considering the effect of lift force, and found that, for sub-micro particles, the lift force could be neglected compared to gravity. Furthermore, they found that when the shear stress was above a certain threshold, the deposition rate became significantly lower. Montassier et al.[18] used an experimental method to investigate the diffusive deposition and thermophoretic deposition in a pipe flow and gave two empirical equations of deposition efficiency for $K_n \geqslant 0.2$ and $K_n < 0.2$. Stratmann et al.[19] built two models to analyze the deposition of particles in a laminar pipe flow considering convection, diffusion and thermophoresis. One model was a highly accurate dimensional model considering the temperature dependence of the material properties, the influence of radial particle number concentration profiles at the tube inlet and of axial heat conduction and axial diffusion. The other model was a non-dimensional model in which a new simplified thermophoretic parameter was introduced. Through non-dimensional analysis, they proposed a simple empirical formula for calculating total thermophoretic deposition efficiency.

Most of the above research concentrated on a single deposition mechanism such as thermophoresis, diffusion or gravity. There have been several studies of particle transport due to multi-mechanisms. Yiantsios and Karabelas[17] described particle transport due to gravity, convection and diffusion. Montassier et al.[18] and Stratmann et al.[19] researched particle deposition with thermophoresis, diffusion and convection. The present work researches particle deposition in a laminar pipe flow considering thermophoresis, gravity, lift force, diffusion, and convection.

2 Governing equations

The analysis assumes that the particle concentration is dilute enough that the aerosol particles do not affect the gas flow field, and that interactions among particles are negligible. For an incompressible gas, and constant properties in a fully developed region of the pipe, the velocity profile of gas along the axis direction is parabolic, and the velocity of gas in the radial direction is zero:

$$u_g(r) = 2u_m\left[1-\left(\frac{r}{r_0}\right)^2\right], \tag{1}$$

where,

$$u_m = \frac{Q}{\pi r_0^2 \rho_g}. \tag{2}$$

For a fully developed temperature field, the gas temperature distribution is only a function of x. Skelland[20] used separation of variables to give the temperature distribution as

$$\frac{T_w - T}{T_w - T_i} = \sum_{j=1}^{j=\infty} B_j \psi_j(r/r_0)\exp\left(-\beta_j^2 \frac{x/r_0}{RePr}\right), \tag{3}$$

where

$$\psi_j(r/r_0) = \sum_{i=0}^{i=\infty} \gamma_{ji}(r/r_0)^i,$$

$$\text{for } i<0,\quad \gamma_i = 0,$$

$$\text{for } i=0,\quad \gamma_i = 1,$$

$$\gamma_{ji} = -\beta_j^2(\gamma_{i-2} - \gamma_{i-4})/i^2,$$

$$\beta_j = 4(j-1) + \frac{8}{3},\qquad j=1,2,3,\ldots,$$

$$B_j = (-1)^{j-1} \times 2.84606\beta_j^{-2/3}.$$

Considering particle transport due to convection, diffusion and external force, the mass conservation equation is

$$\nabla\cdot(\boldsymbol{u}_g n_p) = \nabla\cdot(D_p \nabla n_p) - \nabla\cdot(\boldsymbol{u}_F n_p). \tag{4}$$

The term on the left side of the above equation is the transfer magnitude of particles due to convection. The first term on the right side is the transfer magnitude due to Brownian diffusion, and the second term is the transfer magnitude due to external forces, $\boldsymbol{u}_F$ is the particle velocity produced by external forces.

Since the velocity vector of particles $\boldsymbol{u}_p = \boldsymbol{u}_g + \boldsymbol{u}_F$, eq. (4) is reduced to

$$\nabla\cdot(\boldsymbol{u}_p n_p) = \nabla\cdot(D_p \nabla n_p). \tag{5}$$

The scalar form is

$$\frac{\partial u_p n_p}{\partial x}+\frac{\partial u_p n_p}{\partial r}+\frac{u_p n_p}{r}+\frac{\partial v_p n_p}{r\partial\phi}=D_p\left(\frac{\partial^2 n_p}{\partial x^2}+\frac{\partial^2 n_p}{\partial r^2}+\frac{\partial n_p}{r\partial r}+\frac{\partial^2 n_p}{r^2\partial\phi^2}\right). \tag{6}$$

Considering $\frac{\partial^2 n}{\partial x^2}\ll\frac{\partial^2 n}{\partial r^2}$, the above equation can be transformed to

$$\frac{\partial u_p n}{\partial x}+\frac{\partial u_p n}{\partial r}+\frac{u_p n}{r}+\frac{\partial v_p n}{r\partial\phi}=D_p\left(\frac{\partial^2 n}{\partial r^2}+\frac{\partial n}{r\partial r}+\frac{\partial^2 n}{r^2\partial\phi^2}\right). \tag{7}$$

For an absolute absorption surface, the boundary conditions are

$$r=r_0,\quad n_p=0, \tag{8}$$

$$x=0,\quad n_p=n_i, \tag{9}$$

$$\phi=0 \text{ and } \phi=\pi,\quad \frac{\partial n_p}{\partial\phi}=0. \tag{10}$$

The deposition flux is

$$J=\int_0^L\int_0^{2\pi}\left(-D_p\frac{\partial n_p}{\partial r}\Big|_{r=r_0}+n_p\Big|_{r=r_0}\cdot v_p\right)r_0\mathrm{d}\phi\mathrm{d}x, \tag{11}$$

Because $n\Big|_{r=r_0}=0,$, the above equation becomes

$$J=\int_0^L\int_0^{2\pi}\left(-D_p\frac{\partial n}{\partial r}\Big|_{r=r_0}\right)r_0\mathrm{d}\phi\mathrm{d}x. \tag{12}$$

The deposition efficiency η_d and the transition efficiency η_p are

$$\eta_d=1-\eta_p=\frac{J}{\pi n_i r_0^2 u_m}=1-\frac{\overline{n_o}}{n_i}, \tag{13}$$

where $\overline{n}_o$ is the average concentration of particles at the outlet and is defined by the following equation:

$$\overline{n}_o=\frac{\int_0^{2\pi}\int_0^{r_0}u_p n r\mathrm{d}r\mathrm{d}\phi}{\pi r_0^2 u_m}. \tag{14}$$

3 Particle velocity produced by external forces

When the particles flow with gas in a horizontal pipe, the forces exerted on a particle include thermophoretic force, lift force, drag force of gas and gravity. The terminal velocity of a particle moving in the Stokes region is directly proportional to the external force without the drag force. The constant of proportionality is the particle mobility B. Due to a very little relaxation time for aerosol particles, the assumption that a particles comes instantly to its terminal velocity introduces a negligible error[6]. So the velocity component of particle in the radial direction is expressed as

$$u_p=B\cdot F_{th}+B\cdot\frac{\pi}{6}d_p^3\cdot\rho_p\cdot\left(1-\frac{1}{S}\right)g\cos\phi+B\cdot F_L, \tag{15}$$

and the velocity component in the circumferential direction is

$$v_p = -B \cdot \frac{\pi}{6} d_p^3 \cdot \rho_p \cdot \left(1 - \frac{1}{S}\right) g \sin\phi. \tag{16}$$

According to the definition of particle mobility,

$$B = \frac{\rho_g C_c}{3\pi \nu d_p}, \tag{17}$$

where C_c is the Stokes Cunningham slip correction coefficient, and the slip correction coefficient for a solid spherical particle[23]:

$$C_c = 1 + \frac{\lambda}{d_p}\left[2.34 + 1.05 \exp\left(-0.39 \frac{d_p}{\lambda}\right)\right]. \tag{18}$$

3.1 Thermophoretic velocity

For thermophoresis, there are several famous equations, such as the Brock-Talbot equation[7,8], the Derjaguin-Yalamov equation[21,22], the Cha-McCoy-Wood equation[12,13], and the modified Cha-McCoy-Wood equation[14]. Based on the research of He and Ahmadi, the thermophoresis equations were selected as follows: for $K_n > 2$, the modified Cha-McCoy-Wood equation was selected, and for $K_n \leqslant 2$, the Brock-Talbot equation was employed.

The Brock-Talbot equation is as follows:

$$U_{th} = -\frac{2C_s C_c \nu \left(\frac{k_g}{k_p} + C_t \frac{\lambda}{R_p}\right)\left(\frac{\nabla T}{T}\right)}{\left(1 + 3C_m \frac{\lambda}{R_p}\right)\left(1 + 2\frac{k_g}{k_p} + 2C_t \frac{\lambda}{R_p}\right)}. \tag{19}$$

Reasonable values of C_s, C_t and C_m are 1.17, 2.18 and 1.14, respectively.

The modified Cha-McCoy-Wood equation is

$$U_{th} = -1.15 \frac{\lambda / R_p}{4\sqrt{2} h \left(1 + \frac{\pi_1}{2} \frac{\lambda}{R_p}\right)} \cdot \left[1 - \exp\left(-\frac{hR_p}{\lambda}\right)\right] \cdot \left(\frac{4}{3\pi} \psi \pi_1 \frac{\lambda}{R_p}\right)^{1/2} \frac{C_c k \nabla T d_p}{3\pi \mu d_m^2}, \tag{20}$$

where

$$\psi = 0.28(9\gamma - 5)\frac{c_v}{R}, \tag{21}$$

$$h = 0.22\left[\frac{\frac{\pi}{6}\psi}{1 + \frac{\pi_1}{2}\frac{\lambda}{R_p}}\right], \tag{22}$$

$$\pi_1 = 0.18\left[\frac{\frac{36}{\pi}}{(2 - S_n + S_t)\frac{4}{\pi} + S_n}\right]. \tag{23}$$

3.2 Settling velocity

The settling velocity U_s can be calculated by

$$U_s = \frac{(S-1)\cdot g\cdot d_p^2\cdot C_c}{18\nu}. \tag{24}$$

3.3 Lift velocity

When an aerosol particle is suspended in a shear flow, the fluid exerts a lift force on the particle. For a pipe flow, the Saffman lift force is given as [24]

$$F_L = 6.46\cdot\rho_g(u-u_p)\cdot R_p^2\cdot\left(\frac{\mathrm{d}u}{\mathrm{d}r}\cdot\nu\right)^{1/2}, \tag{25}$$

where $u-u_p$ is the instantaneous velocity difference between the particle and the gas in an axial direction, and can be obtained from the momentum equation. Substituting the axial velocity of a particle into eq. (25) gives the lift force expression:

$$F_L(r) = -6.46u_m\cdot\rho_g\cdot d_p^2\cdot\nu^{1/2}\cdot r_0^{-2}\cdot r\cdot[u(r)-u(r-v_p)]. \tag{26}$$

The particle velocity produced by the lift force is

$$U_L(r) = -0.685C_c\cdot u_m\cdot\rho_g^2\cdot d_p\cdot\nu^{-1/2}\cdot r_0^{-2}\cdot r\cdot[u(r)-u(r-v_p)]. \tag{27}$$

4 Non-dimensional form

Introducing the non-dimensional variables $r^* = \frac{r}{r_0}$, $u^* = \frac{u}{u_{\max}}$, $x^* = \frac{x}{r_0}$, $\theta = \frac{T-T_s}{T_i-T_s}$ and $n^* = \frac{n}{n_i}$, the gas velocity in non-dimensional form is

$$u^* = 1 - r^{*2}. \tag{28}$$

The energy equation of gas flow is

$$Pe\cdot u^*\frac{\partial\theta}{\partial x^*} = \frac{\partial^2\theta}{\partial r^{*2}} + \frac{1}{r^*}\frac{\partial\theta}{\partial r^*}. \tag{29}$$

Pe is the Peclet number, defined as

$$Pe = RePr = \frac{u_m d_0}{\alpha}, \tag{30}$$

$$Re = \frac{u_m d_0}{\nu}, \tag{31}$$

$$Pr = \frac{\nu}{\alpha}. \tag{32}$$

The particle transport equation can be written as

$$\begin{aligned} &Pe\cdot u^*\frac{\partial n^*}{\partial x^*} + Pr\frac{1}{r^*}\frac{\partial\left[r^*(-K_{th}c_{th}{}^* + U_s r_0\cos\phi/\nu + K_L r_0)n^*\right]}{\partial r^*} \\ &\quad - PrU_s r_0\sin\phi/\nu\cdot\frac{\partial n^*}{r^*\partial\phi} = \frac{1}{Le}\left(\frac{\partial^2 n^*}{\partial r^{*2}} + \frac{\partial n^*}{r^*\partial r^*} + \frac{\partial^2 n^*}{r^{*2}\,\partial\phi^2}\right), \end{aligned} \tag{33}$$

where $c_{th}{}^* = \frac{1}{\theta+\theta^*}\frac{\partial\theta}{\partial r^*}$, $\theta^* = \frac{T_s}{T_e-T_s}$, $K_L = \frac{U_L}{\nu}$, Le is the Lewis number, and $Le = \frac{\alpha}{D_p}$. K_{th}

is the thermophoretic coefficient and is defined as

$$U_{\mathrm{th}} = -K_{th} v \frac{\nabla T}{T}. \tag{34}$$

The Brock-Talbot equation employed was

$$K_{th} = \frac{2C_s C_c \left(\frac{k_g}{k_p} + C_t \frac{\lambda}{R_p} \right)}{\left(1 + 3C_m \frac{\lambda}{R_p} \right) \left(1 + 2\frac{k_g}{k_p} + 2C_t \frac{\lambda}{R_p} \right)}, \tag{35}$$

and the MCMW equation was

$$K_{th} = 1.15 \frac{\lambda / R_p}{4\sqrt{2}h(1 + \frac{\pi_1}{2}\frac{\lambda}{R_p})} \cdot \left[1 - \exp\left(-\frac{hR_p}{\lambda} \right) \right] \cdot \left(\frac{4}{3\pi} \psi \pi_1 \frac{\lambda}{R_p} \right)^{1/2} \frac{C_c kTd_p}{3\pi v^2 d_m^2 \rho_g}. \tag{36}$$

For $K_n \leqslant 2$, eq. (35) was selected to calculate K_{th}. For $K_n > 2$, eq. (36) was selected to calculate K_{th}. Considering the continuity at $K_n = 2$, a correction coefficient was introduced into eq. (36).

The boundary conditions are

$$r^* = 1, \quad n^* = 0, \quad \theta = 0, \tag{37}$$

$$x^* = 0, \quad n^* = 1, \quad \theta = 1, \tag{38}$$

$$\phi = 0 \ \text{ and } \ \phi = \pi, \quad \frac{\partial n^*}{\partial \phi} = 0, \tag{39}$$

and the deposition flux of the particle is

$$J = \int_0^{L/r_0} \int_0^{2\pi} \left(-D_p r_0 \frac{\partial n^*}{\partial r^*}\Big|_{r^*=1} \right) r_0 \mathrm{d}\phi \mathrm{d}x^*. \tag{40}$$

5 Computational results

Utilizing the method of finite differences, Patankar[25] implemented the SIMPLER (Revised Semi-Implicit Method for Pressure-linked) algorithm as a computer code for a numerical solution, combining both the transfer and fluid flow problems. During the numerical solution, the Line-by-Line Method was applied. This method is a combination of the TriDiagonal-Matrix Algorithm (TDMA) and the Gauss-Seidel Point-by-Point Method. The mechanism of this method is described in detail in reference [25].

From the particle transport eq. (33), the particle distributions of particles are related to the temperature field of the gas media and also to the physical properties of the gas media and particles. To verify the validity of the computation method, results obtained by the model were compared with experimental data. The experiment conducted by Stratmann et al.[19] was chosen to investigate particle transport due to combined convection, diffusion and thermophoresis, with sodium chloride selected as the particle. The deposition pipe was arranged vertically and the influence of gravity was negligible. By computation, the lift force was very small compared with the thermophoretic force and gravity for a laminar pipe flow. In the following analysis, we neglected the effect of lift force on particle deposition. The comparison is shown in Figure 1. The theoretical results and experimental data were in very good agreement. The maximum deviation of the theoretical result

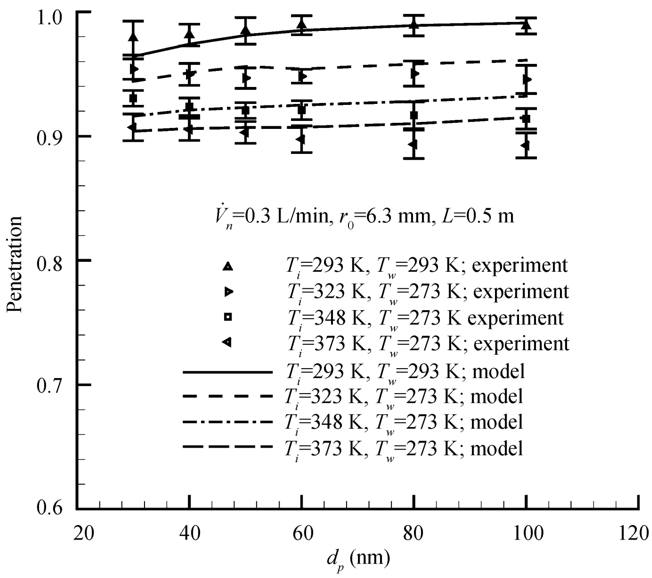

Figure 1 The comparison between the theoretical results and experimental results.

was about 2% from the mean value of the experimental data. When the inlet temperature of the gas was the same as the temperature of the pipe wall, the particle deposition arose from convection and diffusion. For the case of $T_i = T_w = 293$ K, when the particle was small, the theoretical results were slightly lower than the experimental data. This is due to particle diffusion in the axial direction being ignored in the theoretical computation (reference eq. (7)). With the particle deposition in the pipe, the particle concentration continually decreased in the flow direction. For small particles, there was a high diffusion coefficient so that there was some particle diffusion in the axial direction to increase the penetration. This phenomenon also existed in the other analysis cases shown in Figure 1. When the inlet temperature of gas was higher than the temperature of the pipe wall, thermophoretic deposition occurred. In computation, the properties were taken as constant. The characteristic temperature was calculated as the mean of the inlet temperature of the gas and the temperature of the pipe wall. For large particles, the theoretical results were a little higher than the mean value of the experimental data. The deviation increased with the temperature difference between the inlet temperature of the gas and the temperature of the pipe wall. The reasons for this case are as follows.

1) In calculating the thermophoretic coefficient, constant properties were adopted, which introduced deviation. The deviation increased with the temperature difference between inlet temperature of the gas and the temperature of the pipe wall.

2) In theoretical analysis, the effect of gravity was neglected. For the vertical pipe, when gas flowed downwards, the settling velocity increased the lift force to promote the deposition of particles.

3) Increasing the temperature difference between the inlet temperature of the gas and the temperature of the pipe wall, the radial velocity of the particle also increased, which augmented the velocity difference and promoted the particle deposition.

When the pipe was placed horizontally, the deposition mechanisms should include settling. Particle deposition considering settling is shown in Figure 2. For small particles, the penetration considering settling was the same as the penetration without considering settling. For small particles, the Brownian motion was intense, and the settling velocity was low. The main deposition mechanism was diffusion. With increasing particle size, the Brownian motion weakened gradually, but the settling velocity gradually increased. The result was that the deposition amount due to gravity increased and the deposition amount due to diffusion decreased. Without considering settling, the penetration of particle increased monotonically. However, considering settling, the penetration had a maximum.

Figure 2 shows the particle transport considering diffusion, settling and thermophoresis. For small particles, the diffusive and thermophoretic deposition were dominant and increased as particle size decreased. For larger particles, settling was the main deposition mode.

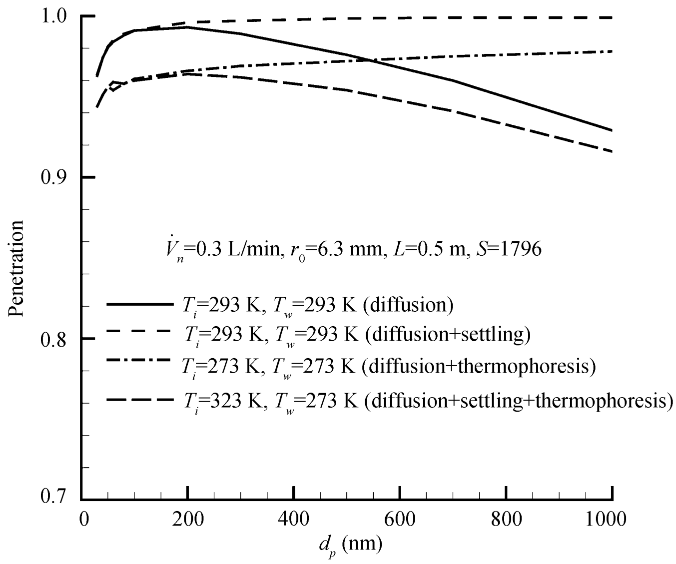

Figure 2 The penetration of aerosol with gravity and without gravity.

Figure 3 shows the non-dimensional concentration distribution at the outlet with a particle diameter of 500 nm. Figure 3(a) shows the concentration distribution in a circumferential direction. Figure 3(b) shows the concentration distribution in a radial direction. In Figure 3(a), the non-dimensional concentrations of a particle vary with angle ϕ at the same non-dimensional radius. When r^* = 0.9, at the top of the pipe (180°$\geqslant\phi$>160°), the particles are dilute and the non-dimensional concentration is less than 0.2. This is due to the settling velocity of particles being higher than the vertical component of thermophoretic velocity so that the vertical velocity of particles flows downwards to engender a dilute zone. With decreasing ϕ, the vertical distance from the pipe wall increases. When a particle leaves the zone, another particle from the upper zone enters this zone, so the particle concentration increases with the decrease of ϕ (160°–100°). When ϕ is about 100°, the supplement for the upper zone is almost equal to the amount of particles leaving this zone. The influence of thermophoresis on particle concentration was visualized. For ϕ > 90°, the vertical component of thermophoretic force points upward, so the particles accumulate at about 100° and form a maximum concentration in a circumferential direction. For ϕ < 90°, the vertical component of thermophoretic force points downward, so the particle concentration decreases with the decrease of ϕ.

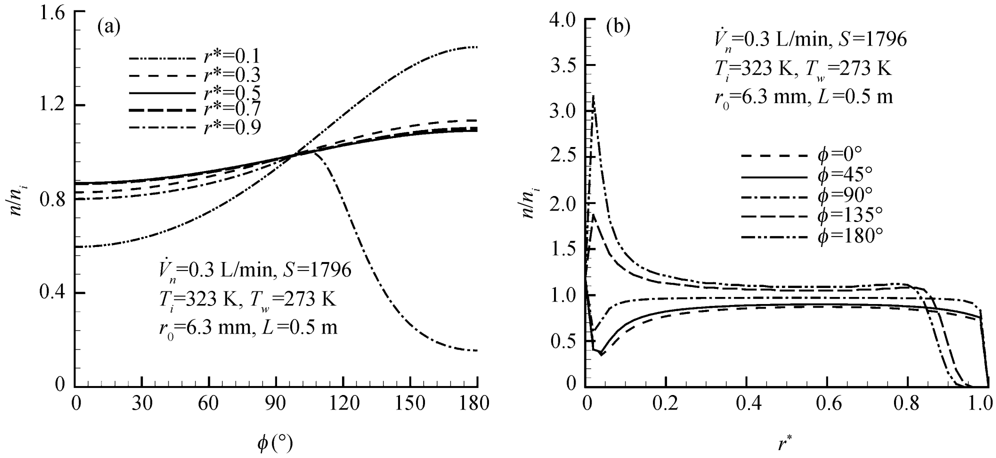

Figure 3 Dimensionless concentration distribution at the outlet (d_p= 500 nm). (a) In a circumferential direction; (b) in a radial direction.

For low r*, the vertical distance from the pipe wall is large. With increasing ϕ ($\phi > 90°$), the vertical component of thermophoretic force also increases, so there is a large accumulation ϕ zone for a low r* and the ϕ associated with maximum concentration also increases, to 180°(see $r^* = 0.7,\ 0.5$, 0.3 and 0.1).

In Figure 3(b), for $\phi > 90°$, an accumulation zone forms in the region $r^*>0.8$, while there is a dilute zone close to the pipe wall. When $\phi = 90°$, the gravity is perpendicular to the radial direction. Particles only bear the thermophoretic force in a radial direction. The concentration distribution is uniform except near $r^* = 0$ and 1 due to the effect of diffusion.

6 Particle deposition by external forces

For large particles, the diffusion coefficient is low, and we can ignore the diffusion deposition. Without considering the lift force, eq. (33) becomes

$$Pe \cdot u^* \frac{\partial n^*}{\partial x^*} + Pr \frac{1}{r^*} \frac{\partial \left[r^* (-K_{th} c_{th}^* + U_s r_0 \cos\phi / \nu) \right]}{\partial r^*} - Pr U_s r_0 \sin\phi / \nu \cdot \frac{\partial n^*}{r^* \partial \phi} = 0. \tag{41}$$

The particle transport equation includes convection, thermophoresis and settling. The above equation can also be solved with the SIMPLER method. Without the SIMPLER method, we can track the particle trajectory to calculate the particle deposition (using the critical particle trajectory method in reference [15]). The critical particle trajectory is shown in Figure 4. A particle starting at the critical radial position r_c at the entrance will be deposited just at the end of the pipe of the length L. This particle is called the critical particle and the trajectory is called the critical trajectory. The corresponding radius at the entrance is called the critical radius. Due to gravity, the particles have a velocity component in a circumferential direction, and the critical radii r_c vary with ϕ.

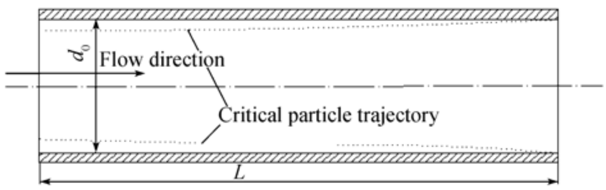

Figure 4 Critical particle trajectory.

According to the motion of the critical particle, the critical particle trajectory is defined as

$$\frac{\mathrm{d}x}{u_p}=\frac{\mathrm{d}r}{v_p}=\frac{r\mathrm{d}\phi}{w_p}. \tag{42}$$

Reference [15] gives the theoretical solution of thermophoretic velocity as

$$U_{th}=f(x)g(r), \tag{43}$$

where

$$f(x)=PrK_{th}\frac{3.36\alpha(T_i-T_w)\exp\left(\frac{-3.36\alpha x}{u_m r_0^2}\right)}{r_0^2\left[T_w+(T_i-T_w)\exp\left(\frac{-3.36\alpha x}{u_m r_0^2}\right)\right]}, \tag{44}$$

$$\begin{aligned} g(r)=0.903r-0.0136r_0\left(\frac{r}{r_0}\right)^2-1.323r_0\left(\frac{r}{r_0}\right)^3+0.355r_0\left(\frac{r}{r_0}\right)^4 \\ +0.581r_0\left(\frac{r}{r_0}\right)^5-0.248r_0\left(\frac{r}{r_0}\right)^6 \end{aligned} \tag{45}$$

Substituting the velocity component of a particle in each coordinate into eq. (42) gives

$$\frac{\mathrm{d}x}{2u_m\left[1-\left(\frac{r}{r_0}\right)^2\right]}=\frac{\mathrm{d}r}{f(x)g(r)+U_g\cos\phi}=\frac{r\mathrm{d}\phi}{-U_g\sin\phi}. \tag{46}$$

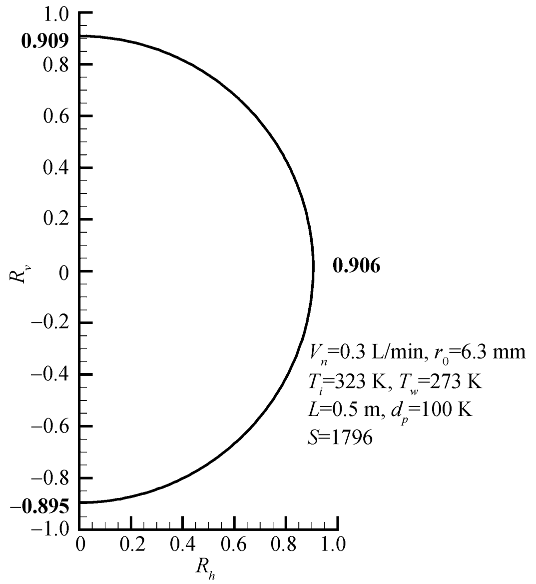

Figure 5 The normalized critical radius for a particle with a diameter of 100 nm.

The above equation can be integrated to obtain the critical radius. Figure 5 shows the critical radii for a particle with a diameter of 100 nm in a 0.5 m long pipe. R_h is the non-dimensional horizontal coordinate normalized by the radius, and R_v is the non-dimensional vertical coordinate normalized by the radius. The figure indicates that at the lower part of the pipe, as the components of thermophoretic force and gravity at the radius are positive, the critical radii are short. At the upper part of the pipe, the component of gravity at the radius is negative, and the critical radii are long. For several special values of ϕ (0°, 90° and 180°), the critical radii are 0.895, 0.906 and 0.909. From the critical radii, the deposition efficiency can be obtained by the following equation:

$$\eta_d = 1 - \eta_p = 1 - \frac{\int_0^{2\pi}\int_0^{r_c} u(r) r n_i r \mathrm{d}r \mathrm{d}\phi}{\int_0^{2\pi}\int_0^{r_c} u(r) r n_i r \mathrm{d}r \mathrm{d}\phi}. \quad (47)$$

The penetration was calculated as 0.966, using the above equation for the case in Figure 5. Using the SIMPLER method, the penetration was calculated to be 0.965 which is in agreement with the results obtained using the critical particle trajectory method.

7 Conclusion

Particle deposition was investigated for a laminar pipe flow, considering convection, diffusion, thermophoresis and gravity. The SIMPLER method was employed to solve the particle transport equation. The concentration profile was obtained for different deposition mechanisms. The variations of penetration of particles (or deposition efficiency) with particle size were also given. The results reveal that for a laminar flow, the influence of lift force on deposition is negligible. For small particles, the main deposition modes are diffusion and thermophoresis. For large particles, the main deposition mode is settling. Therefore, the deposition efficiency has a minimum.

For large particles, the critical particle trajectory method was used to calculate the particle deposition considering thermophoretic force and gravity. The variation of critical radii in a circumferential direction was obtained, and the deposition efficiency of particles was also obtained. The results of calculations using the critical particle trajectory method were in agreement with the results from the SIMPLER method.

Nomenclature

α: thermal diffusivity, m^2/s
B: particle mobility, m/(s·N)
C_c: Stokes Cunningham slip correction coefficient
C_m: momentum exchange coefficient
C_s: thermal slip coefficient
C_t: temperature jump coefficient
c_v: constant volume specific heat, J/(kg·K)
d_0: inner diameter of the pipe, m
d_m: molecule diameter of gas, m
d_p: particle diameter, m
D_p: diffusion coefficient of particles, m^2/s
F_L: lift force, N
F_{th}: thermophoretic force, N
g: gravity acceleration, m/s^2
k: Boltzmann constant, J/K
k_g: gas thermal conductivity,
k_p: particle thermal conductivity, W/(m·K)
K_{th}: thermophoretic coefficient
K_n: Knudsen number
L: pipe length, m
Le: Lewis number
n_i: particle concentration at the inlet, m^{-3}
$\overline{n}_o$: average concentration at the outlet, m^{-3}
n_p: concentration of particles, m^{-3}
Pe: Peclet number
Pr: Prandtl number
Q: mass flow of gas, kg/s
r: radial coordinate, m
r_0: pipe inner radius, m
R_c: critical radius, m
R: idea gas constant, J/(mol·K)
R_p: particle radius, m
Re: Reynolds number
S: density ratio of particle to gas
S_n: normal momentum accommodation coefficient
S_t: tangential momentum accommodation coefficient
T: gas temperature, K
T_i: inlet temperature of gas, K
T_m: mixing-cup temperature, K
T_w: wall temperature, K
$\boldsymbol{u}_F$: velocity vector of particles produced by external forces, m/s
u_g: velocity of gas, m/s
$\boldsymbol{u}_g$: velocity vector of the gas, m/s
u_m: mean velocity of gas, m/s
u_p: velocity component of the particle in the radial direction, m/s
$\boldsymbol{u}_p$: velocity vector of particle, m/s

U_L: particle velocity produced by the lift force, m/s

U_s: settling velocity, m/s

U_{th}: thermophoretic velocity, m/s

v_p: velocity component of the particle in the radial direction, m/s

V_n: volume flow of gas, m^3/s

x: axis coordinate, m

w_p: velocity component of the particle in the circumferential direction, m/s

ρ_g: density of gas, kg/m^3

ρ_p: density of particle, kg/m^3

ϕ: angular coordinate beginning at straight down, °

η_d: deposition efficiency

η_p: transition efficiency

ν: kinematic viscosity of gas, m^2/s

μ: viscosity of gas, kg/(m·s)

γ: specific heat ratio

λ: mean free path of the gas, m

1 Ounis H, Ahmadi G. Comparison of Brownian and turbulent diffusion. Aerosol Sci Technol, 1990, 13(1): 47－53

2 Ounis H, Ahmadi G, McLaughlin J B. Brownian diffusion of submicron particles in the viscous sublayer. J Colloid Interface Sci, 1991, 143(1): 266－277

3 Ounis H, Ahmadi G, McLaughlin J B. Dispersion and deposition of Brownian particles from point sources in a simulation turbulent channel flow. J Colloid Interface Sci, 1991, 147(1): 233－250

4 Li A, Ahmadi G. Dispersion and deposition of spherical particles from point sources in a turbulent channel flow. Aerosol Sci Technol, 1992, 16(4): 209－226

5 Li A, Ahmadi G. Deposition of aerosol on the surface in a turbulent channel flow. Int J Eng Sci, 1993, 31(3): 435－451

6 Hinds W. Aerosol Technology: Properties, Behavior, and Measurement of Airborne Particle. NewYork: John Wiley and Sons Press, 1999

7 Brock J R. On the theory of thermal forces acting on aerosol particles. J Colloid Interface Sci, 1962, 17(8): 768－780

8 Talbot L, Cheng R K, Schefer R W, et al. Thermophoresis of particles in a heated boundary layer. J Fluid Mech, 1980, 101(4): 737－758

9 Tasi C J, Lu H C. Design and evaluation of a plate-plate thermophoretic precipitator. Aerosol Sci Technol, 1995, 22(2): 172－180

10 Li W, Davis E J. Measurement of the thermophoretic force by electrodynamic levitation: Microsphere in air. J Aerosol Sci, 1995, 26(7): 1063－1083

11 Li W, Davis E J. The effect of gas and particle properties on thermophoresis. J Aerosol Sci, 1995, 26(7): 1085－1099

12 Wood N B. The mass transfer of particles and acid vapour to cooled surfaces. J Inst Energ, 1981, 54(419): 76－93

13 Cha C Y, McCoy B J, Thermal force on aerosol particles. Phys Fluids, 1974, 17(7): 1376－1380

14 He C H, Ahmadi G. Particle deposition with thermophoresis in laminar and turbulent duct flow. Aerosol Sci Technol, 1998, 29(6): 525－546

15 Lin J S, Tsai C J. Thermophoretic deposition efficiency in a cylindrical tube taking into account developing flow at the entrance region. J Aerosol Sci, 2003, 34(5): 569－583

16 Tsai C J, Lin J S, Aggarwal S G, et al. Thermophoretic deposition of particles in laminar and turbulent tube flows. Aerosol Sci Technol, 2004, 38(2): 131－139

17 Yiantsios S G, Karabelas A J. The effect of gravity on the deposition of micro-sized particles on smooth surface. Int J Multiph Flow, 1998, 24(2): 283－293

18 Montassier N, Boulaud D, Renoux A. Experimental study of thermophoretic particle dposition in laminar tube flow. J Aerosol Sci, 1991, 22(5): 677－687

19 Stratmann F, Otto E, Fissan H. Thermophoretical and diffusional particle transport in cooled laminar tube flow. J Aerosol Sci, 1994, 25(7): 1305－1319

20 Skelland A H P. Diffusional Mass Transfer. New York: Wiley Press, 1974

21 Yalamov Y. Theory of thermophoresis of large aerosol particles. J Colloid Interface Sci, 1965, 20(6): 555－570

22 Derjaguin B V, Storozhilova A I. Experimental verification of theory of thermophoresis of aerosol particles. J Colloid Interface Sci, 1966, 21(1): 35－58

23 Allen M D, Raabe O G. Slip correction measurements of spherical solid aerosol particles in an improved Millikan apparatus. Aerosol Sci Technol, 1985, 4(3): 269－286

24 Saffman P G. The lift on a small sphere in a slow shear flow. J Fluid Mech, 1965, 22(2): 385－400

25 Patankar S V. Numerical Heat Transfer and Fluid Flow. New York: cGraw-Hill Press, 1980